

# Link Budget Analysis of a Biocompatible Dual-band Implantable Antenna for Intracranial Pressure Monitoring

*Konstantinos A. Psathas, Asimina Kiourti, and Konstantina S. Nikita*

School of Electrical & Computer Engineering, National Technical University of Athens,  
9, Iroon Polytechniou Str., 15780 Zografos, Athens Greece  
[kpsathas@biosim.ntua.gr](mailto:kpsathas@biosim.ntua.gr), [akiourti@biosim.ntua.gr](mailto:akiourti@biosim.ntua.gr), [knikita@ece.ntua.gr](mailto:knikita@ece.ntua.gr)

## Abstract

Next generation (next-gen) Implantable Medical Devices (IMDs) require miniature, high-performance biocompatible antennas. In this study, we numerically assess the telemetry link between a biocompatible dual-band implantable antenna and an external receiver. Two telemetry scenarios are examined: with and without the presence of an intermediate relay antenna. Use of the relay antenna is proposed towards a more stable and reliable telemetry link. Its aim is to improve the energy efficiency of the implant, while limiting the electromagnetic exposure of biological tissues. The antenna is considered to be implanted inside the human head for Intracranial Pressure (ICP) monitoring applications.

## 1. Introduction

Biomedical telemetry has long been used for the early diagnosis, monitoring and treatment of people at risk. Recently, a number of implantable biomedical telemetry systems have been proposed, for applications such as glucose [1] or Intra-cranial Pressure (ICP) monitoring [2, 3], etc. Therefore, sophisticated implantable antennas are required to enable bi-directional telemetry between the implant and the exterior monitoring/control system.

Next-generation Implantable Medical Devices (IMDs) require flexible, miniature, multi-band, wideband, high-gain, and biocompatible implantable antennas, which exhibit low Specific Absorption Rate (SAR) in the surrounding biological tissues. The utmost goal is to provide a high-performance telemetry link, while still preserving patient safety. Implantable antennas are one of the most critical and energy-demanding components of IMDs. Ultra-low power microelectromechanical systems (MEMS), microcontrollers, and sensors can generally be packed within a really small footprint. However, miniaturization of implantable antennas that still maintain adequate radiation performance is a critical challenge.

This work focuses on the radiation performance of a biocompatible dual-band implantable antenna which has recently been proposed for ICP monitoring [2]. The biocompatible encapsulation protects the surrounding tissues and has been found to enhance the exhibited radiation efficiency [4], [5]. Medical data is transmitted in the Medical Implant Communications Service (MedRadio, 401–406 MHz) band. At the same time, the antenna provides an innovative “sleep and wake-up” link in the Industrial Scientific and Medical (ISM, 2400–2480 MHz), which aims to improve the power efficiency of the IMD. Next, we study the quality of the telemetry link that is formed between the implantable antenna and an external monitoring system. Two scenarios are considered: with and without the presence of an intermediate relay antenna. Use of the relay antenna is proposed towards a more stable and reliable telemetry link. Its aim is to improve the energy efficiency of the IMD, while limiting the exposure of human tissues to electromagnetic radiation.

## 2. Models and Methods

### 2.1 Antenna Models

The implantable antenna examined in this study is shown in Fig. 1(a) [2], and it has been designed for dual-band operation in the MedRadio and ISM bands. It features a typical planar inverted-F antenna (PIFA) structure with a radius of 12.2 mm (total volume of 595 mm<sup>3</sup>). A serpentine patch configuration and a shorting pin (S) are used to increase the effective electrical length and consequently shrink its physical size. The structure is coated with Silastic® MDX4-4210 Biomedical Grade Elastomer ( $\epsilon_r = 3$ ,  $\tan\delta = 0.001$ ) for biocompatibility purposes. The biocompatible layer (bio-layer) covers the external surface of the antenna above the ground plane.

The relay antenna used in this study is shown in Fig. 1(b), and it has also been designed to operate in the MedRadio and ISM bands [6]. This antenna features a triangular patch plane and a shorting pin (S), and exhibits a rectangular shape (60 mm x 70 mm) with a total occupied volume of 6.72 cm<sup>3</sup>. Finally, a half-wavelength dipole antenna which operates in MedRadio is selected to serve as the external receiving antenna. All antennas are fed through 50-Ohm coaxial cables (F).

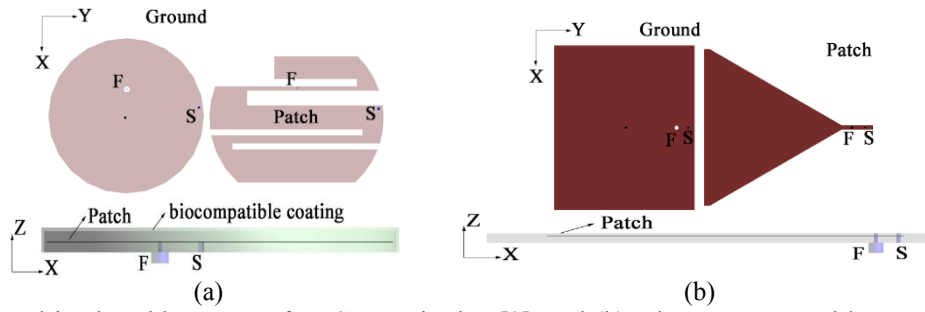


Fig. 1. (a) Dual-band implantable antenna for ICP monitoring [2], and (b) relay antenna used between the implantable and external antennas [6].

## 2.2 Head Model and Numerical Methods

For enhanced accuracy in the derived numerical results, the Duke anatomical head model with compressed ears is considered (part of the Virtual Population by IT'IS) (Fig. 2) [7]. This model includes 45 types of biological tissues, the dielectric properties of which are assumed to be constant within a small window around the center frequency of the MedRadio (403.5 MHz) and ISM (2450 MHz) bands. This assumption accelerates simulations, without degrading the accuracy of the results [8].

FDTD simulations are carried out using the SEMCAD X software by SPEAG [9]. Minimum spatial resolution is set to  $48 \times 73 \times 79 \mu\text{m}^3$  (MedRadio band) and  $47.8 \times 48.3 \times 52.9 \mu\text{m}^3$  (ISM band), while maximum spatial resolution is set to  $29 \times 29 \times 29.5 \text{ mm}^3$  (MedRadio band) and  $9.4 \times 9.8 \times 8.7 \text{ mm}^3$  (ISM band). The grading ratio (maximum ratio of the length of two neighboring cells along an axial direction in the grid) is 1:2, while the gridding ratio relaxation (percentage of local relaxation of the grading ratio to prevent over-refinement in areas with closely spaced baselines) is 10%. The minimum baseline resolution is set to  $0.0001\lambda$  with maximum grid cells (max step) of  $0.07\lambda$ , where  $\lambda$  is the wavelength at the corresponding frequency. The max step satisfies the FDTD spatial step constraint and has conservatively been chosen to reduce potential dispersion errors generated by the non-uniformity of the grid. The Absorbing Boundary Conditions (ABC) are set as Uniaxial Perfectly Matched Layer (U-PML) with low strength (absorption level  $> 90\%$ ) [10]. Gaussian sources are used for the broadband simulations.

## 3. Numerical Results and Discussion

The simulation set-ups are shown in Fig. 2. The upper surface of the implantable antenna is placed 3 mm under the external surface of the head model while the center of the antenna ground plane coincides with the origin of the coordinates system,  $O(0,0,0)$ . The external receiving dipole is placed along the z-axis, as shown in Fig. 2, and can move across the x-axis. The relay antenna is placed as shown in Fig. 2(b), at a distance  $d_3 = 80 \text{ mm}$  from  $O(0,0,0)$  across x-axis.

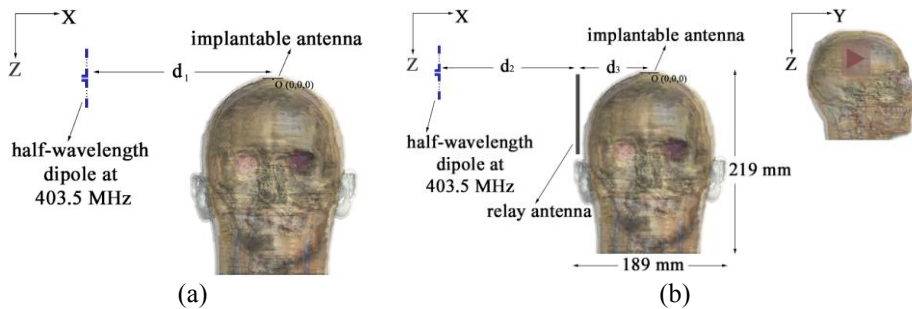


Fig. 2. Simulation set-ups: (a) without the relay antenna, and (b) with the relay antenna.

The reflection coefficient ( $|S_{11}|$ ) frequency responses of the dual-band implantable and relay antennas are shown in Fig. 3. The implantable antenna resonates at 405.5 and 2451.1 MHz with a bandwidth of 16.2 and 89.04 MHz, respectively. The wearable antenna resonates at 407.16 and 2413.24 MHz with a bandwidth of 6.4 and 43.5 MHz, respectively.

The exhibited far-field gain radiation patterns for both antennas are shown in Fig. 4. The implantable antenna exhibits a directional and asymmetrical radiation pattern in both bands (Fig. 4(a)). Maximum far-field gain ( $G_{\text{max}}$ ) values at 403.5 and 2450 MHz are computed as -34.77 and -14.85 dBi, respectively. Asymmetry of the radiation pattern is due to the inhomogeneous dielectric structure of the anatomical head. The wearable antenna exhibits an almost omnidirectional radiation pattern in the MedRadio band, and a directional and asymmetrical radiation pattern in the ISM band, with its main lobe pointing out of the radiation patch (Fig. 4(b)). Maximum far-field gain ( $G_{\text{max}}$ ) values at 403.5 and 2450 MHz are equal to -26.68 and 5.4 dBi, respectively.

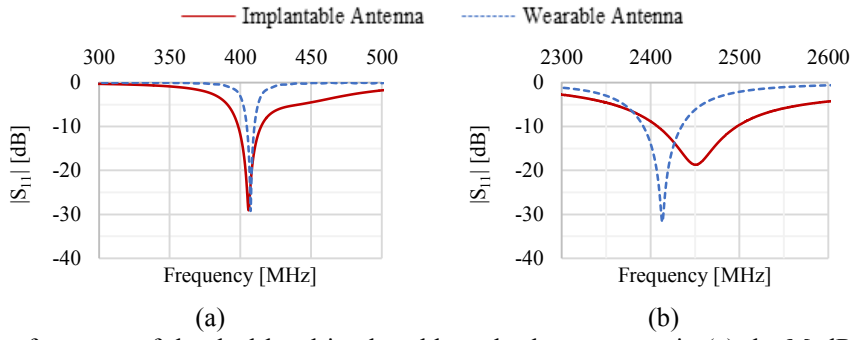


Fig. 3. Resonance performance of the dual-band implantable and relay antennas in (a) the MedRadio and (b) the ISM bands.

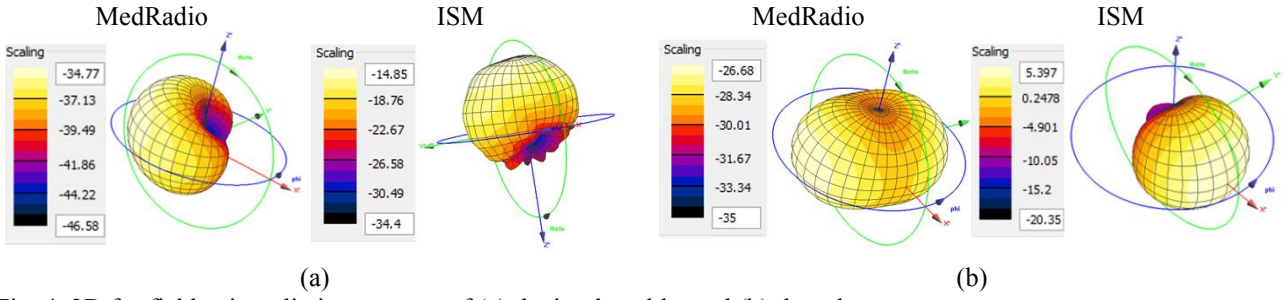


Fig. 4. 3D far-field gain radiation patterns of (a) the implantable, and (b) the relay antennas.

Safety performance of the implantable and relay antennas is further evaluated. The exhibited maximum SAR values averaged over 10 g of tissue in the shape of a cube ( $SAR_{10g}$ ) for the two antennas in the MedRadio and ISM bands are shown in Fig. 5. The latest IEEE C.95.1-2005 safety standard limits the input power to the implantable antenna ( $P_{max}$ ) so that the maximum  $SAR_{10g}$  is less than 2 W/kg [11]. In order to conform with these IEEE guidelines,  $P_{max,impl.}$  should be limited to less than 38.5 mW and 39.8 mW for the MedRadio and ISM bands, respectively. Similarly,  $P_{max,wear.}$  should be limited to less than 1.22 and 0.21 W for the MedRadio and ISM bands. Spatial distributions of the  $SAR_{10g}$  on the coronal plane, where maximum local SAR has been observed, are illustrated in Fig. 6.

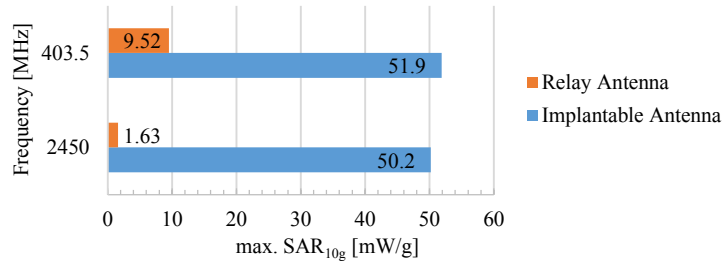


Fig. 5. Maximum  $SAR_{10g}$  produced by each antenna for 1 W input power in MedRadio and ISM band.

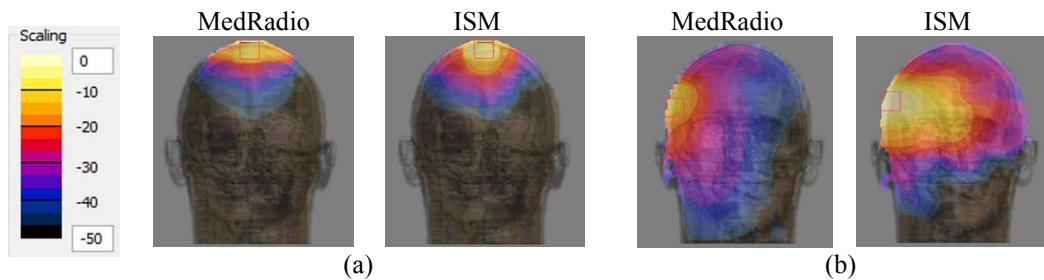


Fig. 6. Distribution of the  $SAR_{10g}$  on the coronal plane where maximum local SAR has been observed for the (a) implantable, and (b) relay antennas (1 W input power). The values are normalized to the maximum  $SAR_{10g}$  calculated for each antenna (Fig. 6). The highlighted box, defines the cube [11] in which the max.  $SAR_{10g}$  is calculated.

Finally, half-duplex communication is studied between the implantable antenna and the external half-wavelength dipole, without (Fig. 2(a)) and with (Fig. 2(b)) the use of the intermediate relay antenna. As part of this study, the relay antenna is placed in close proximity to the head model. However, in a realistic scenario, this antenna could be a patch on the patient's head or part of a wearable band. In the first scenario (Fig. 2(a)), data is transmitted directly from the implantable antenna to the external dipole in the MedRadio band. The corresponding transmission coefficient is computed and shown in Fig. 7. Assuming a net input power of 38.5 mW (15.85 dBm), the received power is calculated as shown in Fig. 7. For a typical receiver sensitivity of -70 dBm, the telemetry link is found to be reliable up to a distance of

6 m between the antennas. In the second scenario (Fig. 2(b)), the transmission coefficient between the implantable and wearable antenna is calculated as -66.7 dBm. Assuming the same receiver sensitivity, the input power for the implantable antenna can be limited to 0.5 mW (or -3.3 dBm) for an inter-antenna separation distance of 6 m. For the sake of completeness, the transmission coefficient between the relay antenna and the exterior dipole is also studied. In this case, and for a receiver sensitivity of -70 dBm, the input power of the relay antenna can be limited to 6.6 mW (or 8.2 dBm) for reliable communication at a distance of 6 m. Based on the above, use of the relay antenna allows for a reduction in the input power to the implanted antenna by a factor of 80. In both scenarios, the wake-up signal is sent to the implanted device using the ISM band.

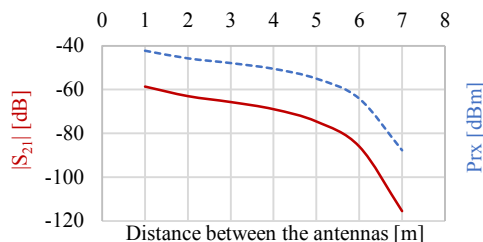


Fig 7. Transmission coefficient ( $|S_{21}|$ ) and received power ( $P_{rx}$ ) versus distance between the implantable antenna and the external dipole without the presence of the relay antenna.

## 4. Conclusion

In this work, we assessed the communication link between a biocompatible dual-band implantable antenna and an external monitoring device, with and without the presence of a wearable relay antenna. A miniature biocompatible implantable antenna placed under the skin of an anatomical head model was considered. It was demonstrated that the use of the relay results in a reduction by a factor of 80 of the power of the implanted antenna required to establish a reliable communication link with the external communication device.

## 5. Acknowledgement

This work has been co-financed by the European Union (European Social Fund, ESF) and national funds, under the project ARISTEIA DEM-II- MED (“Implantable and Ingestible Medical Devices (IIMDs): Optimal- Performance-Oriented Design and Evaluation Methodology”). The authors would like to thank Schmid & Partner Engineering AG (SPEAG) for providing the license for SEMCAD-X software through SEMCAD X for Science agreement.

## 6. References

1. T. Karacolak, A.Z. Hood, and E. Topsakal, “Design of a Dual-Band Implantable Antenna and Development of Skin Mimicking Gels for Continuous Glucose Monitoring,” *IEEE Transactions on Microwave Theory and Techniques*, 2008, vol. 56, pp. 1001-1008.
2. A. Kiourti, K. A. Psathas, J. R. Costa, C. A. Fernandes, and K. S. Nikita, “Dual-Band Implantable Antennas for Medical Telemetry: A Fast Design Methodology and Validation for Intra-Cranial Pressure Monitoring,” *Progress in Electromagnetics Research*, 2013, vol. 141, pp. 161-183.
3. R. Warty, M. R. Tofighi, U. Kawoos, and A. Rosen, “Characterization of Implantable Antennas for Intracranial Pressure Monitoring: Reflection by and Transmission Through a Scalp Phantom,” *IEEE Transactions on Microwave Theory and Techniques*, 2008, vol. 56, pp. 2366-2376.
4. F. Merli, B. Fuchs, J. R. Mosig, and A. K. Skrivervik, “The Effect of Insulating Layers on the Performance of Implanted Antennas,” *IEEE Transactions on Antennas and Propagation*, vol. 59, pp. 21-31, 2011.
5. K. A. Psathas, A. Kiourti, and K.S. Nikita, “Biocompatibility of Implantable Antennas: Design and Performance Considerations”, *8th European Conference on Antennas and Propagation (EuCAP)*, 2014, Hague, Netherlands (to appear).
6. A. Kiourti, J. R. Costa, C. A. Fernandes, and K. S. Nikita, “A Broadband Implantable and a Dual-Band On-Body Repeater Antenna: Design and Transmission Performance”, *IEEE Transactions on Antennas and Propagation*, 2014 (to appear).
7. A. Christ, et al., “The Virtual Family--development of surface-based anatomical models of two adults and two children for dosimetric simulations,” *Phys Med Biol*, 2010, vol. 55, pp. 23-38.
8. A. Kiourti, M. Christopoulou, and K. S. Nikita, “Performance of a novel miniature antenna implanted in the human head for wireless biotelemetry”, *IEEE International Symposium on Antennas and Propagation (APSURSI)*, 2011.
9. Schmid & Partner Engineering AG (SPEAG), “SEMCAD X, Ver. 14.8,” 2013.
10. S. D. Gedney, “An anisotropic perfectly matched layer-absorbing medium for the truncation of FDTD lattices,” *IEEE Transactions on Antennas and Propagation*, 1996, vol. 44, pp. 1630-1639.
11. IEEE, “IEEE Standard for Safety Levels With Respect to Human Exposure to Radio Frequency Electromagnetic Fields, 3 kHz to 300 GHz,” *IEEE Std C95.1-2005*, 2005.